A Combined CFD/Potential Flow Simulation Method for Prediction of Hydrodynamic Maneuvering Forces

Paul F. White, Robert F. Beck, Kevin J. Maki, and Dominic J. Piro

Department of Naval Architecture and Marine Engineering
University of Michigan, Ann Arbor, MI, 48109 USA
pfwhite@umich.edu

INTRODUCTION

Computational Fluid Dynamics (CFD) has become increasingly used as a design tool for ships and offshore structures. Although CFD captures more relevant physics than traditional Boundary Element Methods (BEM), the improved accuracy comes at a cost. CFD simulations are both computationally intensive and time consuming to complete. At the University of Michigan are working on developing more efficient CFD methods while not sacrificing the advantageous features.

Methods utilized for evaluation of a ship's maneuvering capabilities in calm water are generally grouped into two categories; 1) Abkowitz [1] methods requiring an experimental test campaign, and 2) analytic/numerical methods. The Abkowitz methods derive hydrodynamic forces - either for the whole ship/rudder/propeller system or for some subset of components - as Taylor series expansions about a base operating condition. With the coefficients, the fluid forcing is determined for the equations of motion and they can be solved in real time. The method generally manages to capture hull/propeller/rudder interactions and, once the coefficients have been determined, has proven to accurately and efficiently predict some maneuvering responses in calm water. The method is challenged when the forces are evaluated for an operating condition that is dissimilar from the experimental base operating condition.

The analytic/numeric approaches can use CFD, potential flow, experimental data, or some combination. For example, the Maneuvering Modeling Group (MMG) models derive hydrodynamic forces from a combination of experimental data and/or analytical formulae. Typically the experimental force coefficients are determined independently and interactions are described through standard hull/propeller matching methods. The MMG method has been extended to include wave forces through use of the BEM [5, 6, 7]. Challenges encountered with the modular MMG method are that empirical estimates for various components of the force and their interaction are required.

The primary goal of this research is to develop a numerical method motivated by the previous MMG theories that will have comparable accuracy to the Abkowitz methods without the need for a costly experimental campaign. Further, the aim of the method is to achieve better prediction in the operating conditions not captured by the experiment through use of CFD, such as capturing separation effects in the flow. While CFD exists as an accurate alternative to model testing, resolving the free surface is often too costly for use in the design phase. This research proposes a combination method where the BEM and single-phase Unsteady Reynolds-Averaged Navier Stokes (URANS) equations are solved simultaneously. In this way, interaction between the hull and rudder can be simulated directly through the CFD and the wave modeling is effectively handled by the BEM. The work presented herein does not address propulsive forces but does attempt to capture hull/rudder interaction. Results from the proposed method are compared against experimental data for a forced motion Planar Motion Mechanism (PMM) test with attached rudder and rotating propeller [4]. The long-term goal is a co-simulation model including the propeller for large amplitude horizontal plane maneuvering in waves.

METHOD

The method presented here utilizes CFD to solve the equations of fluid motion for a single-phase incompressible, viscous fluid. The fluid pressure and viscous forces are derived from the equations of fluid motion solved on a grid moving with a prescribed PMM maneuver. The total fluid force on the body from the CFD, denoted $\vec{\mathbf{F}}_{\text{URANS}}$, is one component contributing to maneuvers in the horizontal plane and becomes an increasingly better estimate for low Froude number maneuvers. The forcing from radiated waves is handled more efficiently by the BEM and is denoted $\vec{\mathbf{F}}_{\text{mem}}$. This work proposes a combination of the two force components to reconstruct the total hydrodynamic force encountered during a PMM maneuver in calm water.

The combination procedure employs CFD to predict frictional resistance and double-body pressure. These components of force are calculated from the conservation laws for mass and momentum written in Arbitrary Eulerian Lagrangian form. These equations are solved in an Earth-fixed frame for a single-phase fluid with

Reynolds stresses modeled using a two-equation $k - \omega$ SST turbulence model. The solution of this system of equations is referred to within this work as the Unsteady Reynolds-Averaged Navier-Stokes equations as shown in Equation 1.

$$\int_S \vec{\mathbf{U}}_{\text{rel}} \cdot \hat{n} \, dS = 0$$

$$\frac{\partial}{\partial t} \int_V \vec{\mathbf{U}} dV + \int_V \nabla \cdot \vec{\mathbf{U}} \vec{\mathbf{U}}_{\text{rel}} dV = -\int_V \frac{\nabla p}{\rho} dV + \int_V \nabla \cdot \nu_{\text{eff}} \left[\nabla \vec{\mathbf{U}} + \nabla \vec{\mathbf{U}}^T \right] dV + \int_V \vec{\mathbf{f}}_B dV \tag{1}$$

The conservation equations are solved using the open source toolkit OpenFOAM, which uses a cell-centered finite volume discretization on arbitrary polyhedral cells. The CFD mesh used in the current simulations contains a discretized rudder but currently no representation of a propeller; a propeller model will be added in the future. The total hydrodynamic force on the body is computed as in Equation 2, where $\overline{\overline{\sigma}}$ is the total stress tensor.

$$\vec{\mathbf{F}}_{\text{URANS}} = \int_S \overline{\overline{\sigma}} \cdot \hat{n} \, dS \tag{2}$$

The wave radiation forces are calculated by a higher-order BEM, Aegir [2], which utilizes higher-order representations of the geometry and velocity potential. Aegir is a direct BEM and distributes sources and dipoles on the body-mean position and across the calm water surface and numerical beach. The total perturbation potential is linearized about the free-stream (Neumann-Kelvin linearization) and is split into two components to solve for the fluid response to the forced-motions problem. In Aegir, the impulsive part of the potential that handles unsteady body motions is called the local potential and is denoted ϕ_{loc}. The component satisfying the free surface conditions is referred to as the memory flow potential and denoted ϕ_{mem}. The total perturbation potential is linearly decomposed according to Equation 3.

$$\Psi(\vec{x}, t) = \phi_{\text{loc}}(\vec{x}, t) + \phi_{\text{mem}}(\vec{x}, t) \tag{3}$$

Due to the linearization of the problem, each potential is subject to the same form of the Boundary Integral Equation (BIE), but with different boundary conditions, forming two unique Boundary Value Problems (BVP). The BIE for the direct solution of the total perturbation potential is of the general form shown in Equation 4.

$$2\pi \Psi(\vec{x}) - \iint_{S_B \cup S_F} \frac{\partial \Psi(\vec{x}')}{\partial n} G(\vec{x}'; \vec{x}) dS(\vec{x}') + \iint_{S_B \cup S_F} \frac{\partial G(\vec{x}'; \vec{x})}{\partial n} \Psi(\vec{x}') dS(\vec{x}') = 0 \tag{4}$$

In this work, the body boundary condition is linearized about the body-mean position. In the frame of the body's mean position the unit direction $\hat{i}$ is positive towards the bow, $\hat{j}$ is positive to port, and $\hat{k}$ is vertically up. The displacements from the mean are the six degrees of freedom surge, sway, heave, roll, pitch, and yaw. The translational degrees of freedom are denoted $\vec{\xi}_T = (\xi_1, \xi_2, \xi_3)$ and the rotational degrees of freedom as $\vec{\xi}_R = (\xi_4, \xi_5, \xi_6)$, such that the first order displacement vector at any point on the body surface is $\vec{\delta} = \vec{\xi}_T + \vec{\xi}_R \times \vec{x}$. Using the Neumann-Kelvin approximation, the body boundary conditions are satisfied on the mean position of the body, whose surface is denoted $S_{\overline{B}}$ and moves at constant speed U_c. As a result, the velocity of the body-mean position is $\vec{\mathbf{W}} = U_c \hat{i}$ where U_c is the carriage speed. The boundary conditions to be met by ϕ_{loc} are:

$$\frac{\partial \phi_{\text{loc}}}{\partial n} = \sum_{j=1}^{6} \left(\frac{\partial \xi_j}{\partial t} n_j + \xi_j m_j \right) \quad \text{on S}_{\overline{B}} \tag{5}$$

$$\phi_{\text{loc}} = 0 \quad\quad\quad\quad\quad \text{on z= 0}$$

where

$$(n_1, n_2, n_3, n_4, n_5, n_6) = (\hat{n}, \vec{x} \times \hat{n})$$

$$(m_1, m_2, m_3) = (\hat{n} \cdot \nabla) \vec{\mathbf{W}} = (0, 0, 0)$$

$$(m_4, m_5, m_6) = (\hat{n} \cdot \nabla) \left(\vec{x} \times \vec{\mathbf{W}} \right) = (0, +U_c n_3, -U_c n_2)$$

The memory flow BVP governs the radiated and diffracted wave fields. In this work, the calm water maneuver is prescribed and only the radiation problem is solved. The BVP for ϕ_{mem} is governed by the body boundary condition and the free surface boundary conditions in Equations 6 and 7.

$$\frac{\partial \phi_{\text{mem}}}{\partial n} = 0 \text{ on S}_{\overline{B}} \tag{6}$$

The kinematic and dynamic free surface boundary conditions are listed in Equation 7, where ζ is the radiated wave elevation and ϕ_{mem} is the memory flow velocity potential.

$$\frac{\partial \zeta}{\partial t} - (\vec{\mathbf{W}} \cdot \nabla)\zeta = \frac{\partial \phi_{\mathrm{loc}}}{\partial z} + \frac{\partial \phi_{\mathrm{mem}}}{\partial z} \qquad \text{on z= 0}$$
$$\frac{\partial \phi_{\mathrm{mem}}}{\partial t} - (\vec{\mathbf{W}} \cdot \nabla)\phi_{\mathrm{mem}} = -g\zeta \qquad \text{on z= 0} \tag{7}$$

The radiated wave force is obtained by integrating the pressure from the memory flow velocity potential over the body-mean position as in Equation 8.

$$\vec{\mathbf{F}}_{\mathrm{mem}} = -\rho \int_{S_{\overline{B}}} \left(\frac{\partial}{\partial t} - (\vec{\mathbf{W}} \cdot \nabla) \right) \phi_{\mathrm{mem}} \cdot \hat{n} \, dS \tag{8}$$

RESULTS

The KRISO Container Ship (KCS) [3] is the chosen hull for this study. A 1/52.67 geosim of $L_{pp} = 4.367$ m is simulated and commanded through two PMM maneuvers. The first maneuver is a pure sway maneuver with sway amplitude $\xi_2 = 0.127$ m. The second PMM maneuver is a pure yaw maneuver with sway amplitude $\xi_2 = 0.297$ m and yaw amplitude $\xi_6 = 4.7$ deg. Both PMM maneuvers are executed with a period of 13.33 seconds and at Froude number $Fn = 0.26$. In both cases the time series for each individual force component - the total force from the single-phase URANS and the force from the memory flow BVP - is plotted in addition to the sum of components and compared with experimental data submitted by Force Technology to the SIMMAN 2014 Workshop [4].

Pure Sway Maneuver The force and moment time series are shown for three full cycles of the pure sway maneuver in Figure 1 and compared to the one cycle of reported experimental data [4]. The experimental data was phased by synchronizing the recorded experimental motions with the forced motions that were numerically simulated. The total force from the URANS simulation shows it to be in phase with the derived experimental
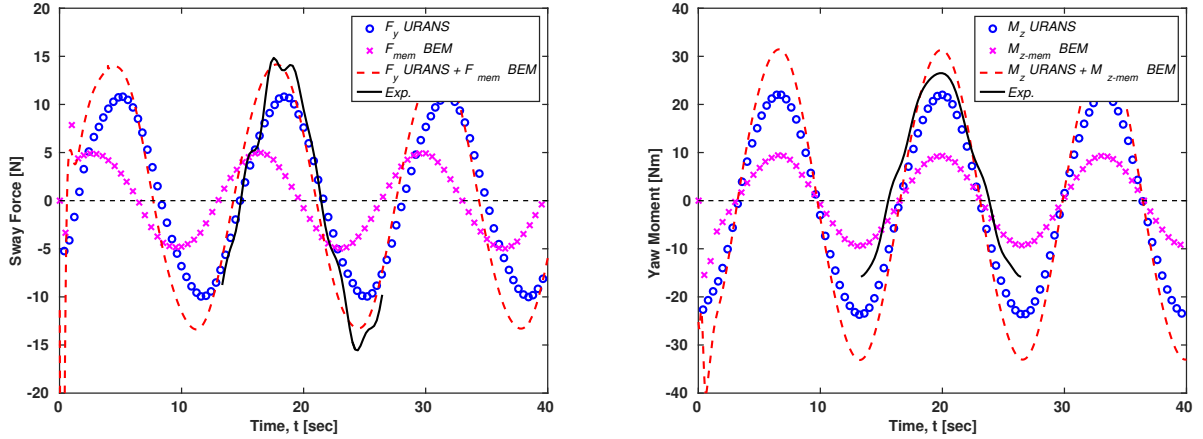

Figure 1: Hydrodynamic force and moment time series for pure sway PMM.

hydrodynamic sway force and nearly represents the entire hydrodynamic response. The memory component of force from the BEM has a small phase difference relative to the CFD and, when added to the URANS results, produces a result close to the maximum measured sway force. The combination of the CFD and wave radiation forces slightly overpredicts the maximum moment and predicts almost double the minimum moment. It is noteworthy that the experiments featured a rotating propeller which was controlled to maintain constant rpm. The propeller could account for some of the asymmetry in hydrodynamic moment observed in the experimental data.

Pure Yaw Maneuver The force and moment time series are shown for three full cycles of the pure yaw maneuver in Figure 2 and compared to the one cycle of reported experimental data [4].

The sway force from CFD is transformed to the ship-fixed frame and plotted with the memory flow component of force from the BEM. The addition of force components reproduces a sway force time series in the ship-fixed

frame that is very comparable to the measured response, with the exception of a higher frequency component noticeably present in the experimental data. The cause of the higher frequency is unknown at present. The hydrodynamic moment from the combined CFD/BEM forcing produces a comparable minimum yaw moment but there is significant asymmetry again in the experimental data. The predicted moment does not manage to capture this asymmetry and underpredicts the maximum yaw moment.
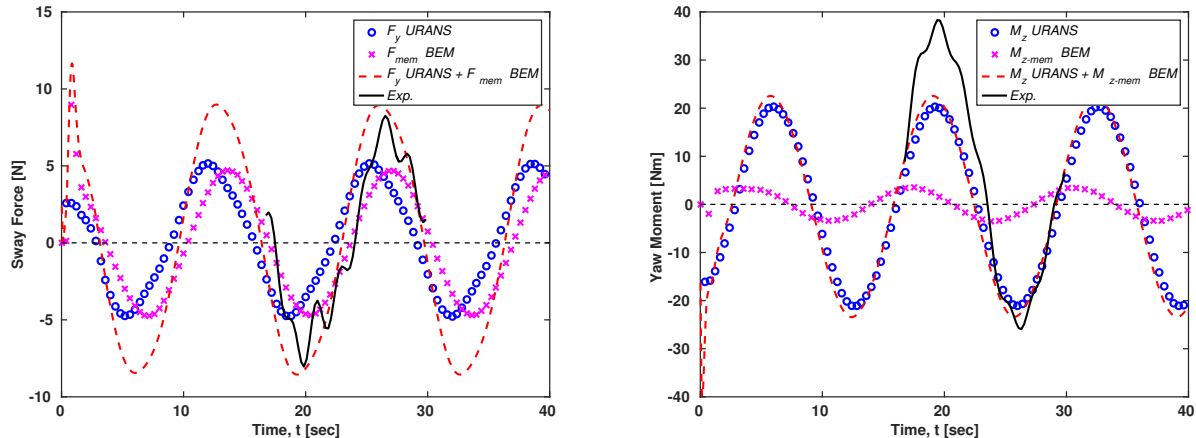

Figure 2: Hydrodynamic force and moment time series for pure yaw PMM.

The authors noted an inconsistency in the presented approach that will be corrected in time for the Workshop. The single-phase URANS simulations impose zero vertical velocity on the calm water plane and so the pressure and viscous forces predicted from the CFD are effectively a zero Froude number approximation. The forces from the local flow BVP were removed from the total force extracted from Aegir. However, the local forces represent the infinite frequency added mass and damping forces as is evident by the definition of the local flow BVP in Equation 5. The added mass and damping due to the waves are calculated relative to the infinite frequency limit to produce the total added mass and damping.

The method explained herein is restricted to small amplitude forced motions due to the formulation within Aegir. A strategy to extend the formulation to handle large amplitude maneuvers in the horizontal plane will be presented at the Workshop. To achieve this, the body boundary condition due to slowly varying horizontal plane maneuvers must be satisfied by a zero Froude number approximation in Aegir so that wave forces extracted from the memory flow BVP are those relative to zero frequency added mass and damping. In the updated method, the URANS and basis flow will both satisfy consistent double-body problems, and the wave flow will be a perturbation.

REFERENCES

[1] M.A. Abkowitz. Lectures on ship hydrodynamics - steering and maneuvrability. *Hydro- and Aerodynamics Laboratory Report*, Lyngby. Denmark. Report No. Hy-5

[2] D.C. Kring. Time domain ship motions by a three-dimensional Rankine panel method. *PhD thesis, Department of Ocean Engineering, Massachusetts Institute of Technology*, 1994.

[3] W.J. Kim, S.H. Van, D.H. Kim. Measurements of flows around modern commercial ship models. *Experiments in Fluids*, 31:567–578, 2001.

[4] J.F. Otzen, C.D. Simonsen. editors. Proceedings SIMMAN 2014 Workshop, Copenhagen, Denmark, December 2014.

[5] M. Seo, Y. Kim. Numerical analysis on ship maneuvering coupled with ship motion in waves. *Ocean Engineering*, 38:1934–1945, 2011.

[6] R. Skejic. Maneuvering and seakeeping of a single ship and of two ships in interaction. *PhD thesis, Department of Marine Technology, Norwegian University of Science and Technology*, 2008.

[7] R. Subramanian, R. Beck. A time domain strip theory approach to maneuvering in a seaway. *Ocean Engineering*, 104:107–118, 2015.